DIAGNOSTYKA, 2024, Vol. 25, No. 4

e-ISSN 2449-5220
DOI: 10.29354/diag/195293

DETECTION AND CLASSIFICATION OF AIR GAP ECCENTRICITY FAULT IN INDUCTION MACHINE USING ARTIFICIAL INTELLIGENCE TECHNIQUES

Moutaz Bellah BENTRAD [1], Adel GHOGGAL [1], Tahar BAHI [2]

[1] Electrical Engineering Department, Electrical Engineering Laboratory of Biskra (LGEB)
University of Biskra, P.O Box 145, 07000, Biskra, Algeria
[2] Electrical Engineering Department, Laboratory of Automation and Signals of Annaba (LASA)
Badji Mokhtar-Annaba University,P.O Box.12, Annaba, 23000 Algeria
* Corresponding author, e-mail: moutazbellah.bentrad@univ-biskra.dz

Abstract

This paper employs artificial intelligence to diagnose induction machine health by detecting air gap eccentricity under varied conditions. It addresses Model-Based Method and conventional MCSA techniques limitations, requiring extensive model knowledge. The proposed technique relies on stator current signals, simplifying data acquisition. Using Root Mean Square and raw data using the three phases of stator current from a multi winding model of a squirrel cage induction machine. The study emphasizes on employing classification and regression tasks for supervised learning as a non-model-based approach by applying several models and classifiers to choose the best one for the monitoring task. This approach allows online diagnosis, detecting defects early, even under weak load conditions by conduction a multiclassification technique for each class of the dataset. The paper's strength lies in its holistic analysis of signal fluctuations, categorizing faults based on nature and location. Overall, the proposed algorithm for the classification which is Decision Trees achieved an overall accuracy surpassing 80% against other classifiers, and for the regression task Random Forest outperformed by delivering the least values of loss error with 0.014 using mean square error evaluation metric and achieving a 98.6% accuracy.

Keywords: induction machine, fault detection, diagnosis, artificial intelligence, machine learning

List of Symbols/Acronyms

AI –Artifcial Intelligence;
ANN –Artificial Neural Network;
FFT – Fast Fourier Transform;
IM –Induction Machine;
HAG –Healthy Air Gap;
HLC –Heavy Load Condition;
MBM –Model-based methods;
MCSA –Motor Current Signature Analysis;
ME –Mixed Eccentricity ;
ML – Machine Learning ;
MLC –Medium Load Condition ;
MWM –Multi-Winding Model ;
NMBM –Non-Model-Based Methods;
RMS –Root Mean Square;
SE –Static Eccentricity;
f_V – viscosity friction coefficient (Kg/m.s);
I_{bk}–current of the bar k (A);
I_{rk}–current of the rotoric loop k (A);
I_r –current of rotor current loop (A);
J –index of rotor current loop;
J_T-total moment of inertia (Kg.m^2);
L_b – leakage inductance of a rotor bar (H);
L_e – leakage inductance of a short-circuit portion (H);
L_{sc} –stator cyclic inductance (H);
L_{sr}- mutual inductances stator and the rotor meshes (H);
N_r –number of bars ;
R_b –rotor bar resistance (Ω);
R_e –short-circuit ring resistance (Ω);
T_e –electromagnetic torque (N.m);
T_r –resistant torque (N.m);
V_r–rotor circuit voltage (V);
V_s–stator circuit voltage (V);
ψ_r–total flux through rotor winding (Wb);
ψ_s–total flux through stator winding (Wb).

1. INTRODUCTION

Induction motors (IMs) are integral to the industrial sector, serving essential functions in mechanical power production, manufacturing, and transportation. They are extensively utilized in a range of applications such as pumps, compressors, fans, machine tools, cranes, conveyors, and electric vehicles. Globally, more than half of the generated electrical energy is employed by motors, with IMs being the primary consumers, accounting for approximately 60% of industrial electricity usage [1]. In numerous industries, the seamless

Received 2024-01-19; Accepted 2024-10-24; Available online 2024-10-28

collaboration of machines is crucial, and the expenses associa ted with unforeseen breakdowns are substantial. In such scenarios, the disruptions of machines in operation often result in significant losses in the production process, surpassing both the expenses incurred for machine repairs and the initial costs of the machines [2]. Hence, it is crucial to proactively identify potential defects in these systems using either traditional or modern methods. This proactive approach enables monitoring and control, facilitating preventive measures to detect and avert sudden incidents or accidents on the machines [3]. Various signal processing techniques have been developed for detecting faults in IM [4]. Initially, factors such as temperature, noise, and vibration signals are considered for fault diagnosis.

The most common type of fault, accounting for 40% of cases, is related to bearing issues. Bearings consist of two rings separated by a series of balls. Any flaws in the balls or inconsistencies in the rings can cause mechanical vibrations, affecting the machine's rotational behaviour. Additionally, stator faults are quite frequent, usually starting as minor issues between turns that can escalate into major phase-to-phase or phase-to-ground faults. [5]. Rotor faults, occurring at a rate of 10%, are less frequent compared to other types. These faults may result from either mechanical or electrical failures. Electrical failures causing thermal increases can lead to rotor bar defects or breakage. Conversely, mechanical problems such as load imbalance or shaft misalignment can harm both bearings and their housing [6, 7]. Additionally, these issues, along with bearing faults, are connected to air gap eccentricity.

Fault diagnosis involves the identification and classification of abnormalities within a system. Two primary methodologies are employed: model-based methods (MBM) and non-model-based methods (NMBM). Model-based approaches utilize mathematical models of the system for fault diagnosis, but obtaining precise models can be challenging due to the inherent nonlinearity of systems. NMBMs, alternatively, rely on measurements, empirical knowledge, or detailed examinations of the system. This category encompasses techniques such as thresholding, expert systems, and the application of artificial intelligence this latter would be used in this research [8].

Motor Current Signature Analysis (MCSA) is among the prominent MBMs extensively employed for monitoring and diagnosing IMs. It leverages spectrum signatures to identify various fault types [9], incorporating techniques like the Fast Fourier Transform (FFT). Nonetheless, FFT's effectiveness and precision are compromised by its time-domain constraints and challenges with nonlinear and non-stationary signals. To address these limitations of FFT, advanced signal processing techniques such as Wavelet Transform (WT) [10], Hilbert Transform (HT) [11], and Short Time Fourier Transform (STFT) [12] are employed. Detecting frequencies related to defects becomes challenging when employing a short acquisition time due to spectral leakage, represented by side lobes. Researchers often address this challenge by using window filters to overcome side lobe leakage, although this approach may result in some loss of information in the obtained results [13].

The dedicated work in this paper aims to use the artificial intelligence techniques through applying multiple machine learning algorithms to be able to detect, identify and localize air gap eccentricity (static and mixed) in the induction machine and gives the modelling details of a three-phase induction motor suffering from static and mixed air gap eccentricity condition under different load conditions. To achieve this, we adopted the multi-winding model (MWM) because it is crucial in fault detection for electrical machines as it improves fault localization, identification, sensitivity, monitoring capabilities, and provides diagnostic insights. By considering each winding separately, the model enables a more accurate and detailed analysis of faults, leading to more effective maintenance and improved machine performance. Naturally, the machine's airgap is not perfectly smooth (initial manufacture imperfections, aging phenomenon, slotting effects…). Consequently, when either static or dynamic fault eccentricity arises, a mixed eccentricity behavior is evident. This is characterized by the recognizable amplitude modulation of the line current at the rotational speed. The basic fault in induction machines, that enclose a major proportion of the machine's defects, is the air-gap eccentricity [14]. Acquisition of the stator current signals obtained by simulating the model for different eccentricity conditions with different functioning profiles. Through the analysis of signal fluctuations accompanying defected machines, the machines will be classified based on the nature and location of the fault. The premise of adopting this paper's proposed technique is to perform a multiclassification process using regression and classification the latter's technique which is Decision Trees achieved an overall accuracy surpassing 80% against other classifiers, and for the regression task Random Forest outperformed by delivering the least values of loss error with 0.014 using mean square error evaluation metric and achieving a 98.6% accuracy.

1.1 Related works

Rouaibia et al in [15], presented two methods to detect air gap eccentricity faults and evaluate its severity by monitoring stator current using Park vector method and discrete wavelet transform in order to distinguish the healthy from the faulty machine, the proposed dynamic model is based on magnetically coupled coils to simulate the behaviour of eccentricity defect.

Maamar et al in [16], investigated the application of continuous wavelet transform in feature extraction and then compared the classification of a multi-layer perceptron neural network algorithm across various cases on vibrational data signal for misalignment defect in three phase induction machine.

Chouidira et al in [17] proposed a method to detect broken rotor bars and inter turn short circuits, by using root mean square (RMS) values extracted from simulating a multi winding model of IM and used it as an input to train an artificial neural network (ANN) algorithm capable of detecting and localizing these defects.

Saucedo et al in [18] conducted a time and frequency domain analysis for a combination of a vibration and current signal of a rotor related defect (bearing) in order to extract statistical features used to train a machine learning algorithm by using ANN classifier to diagnose multiple fault severities

By investigating the literature in the diagnosis of air gap eccentricity and rotor related faults, it became a necessity to employ stator current signal data with artificial intelligence algorithms to detect air gap eccentricity defect and its types under various operating conditions to ensure a strong monitoring performance and avoid undesirable breakdowns.

2. INDUCTION MACHINE FAULTY MODEL

2.1 Multi Winding Model

Figure 1 represents the rotor of an induction cage machine assimilated to a polyphase winding where each mesh is made up of two adjacent bars and two short-circuit ring portions. The stator circuit is composed of a three-phase winding which can be placed in the stator slots in different ways thus defining the type of winding adopted [19, 20].However, within the framework of the study of the detection and localization of possible faults which occur in the IM, the MWM well proven reliability describes the rotor as a set of loops interconnected between them, each formed by two adjacent bars and which end up with the portions of rings which connect them.

Considering the MWM at the induction cage machine, figures 1 and 2, respectively rotor multi-winding scheme, representation of a rotor loop from which we can see that each bar and each rotor ring, is modeled by an inductance and a resistance.

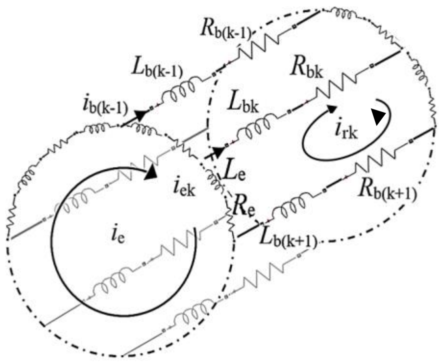

Fig. 1. Rotor multi-winding scheme

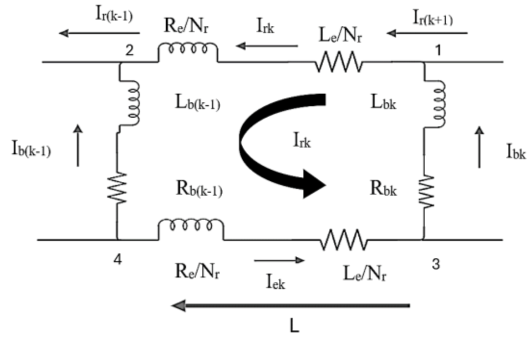

Fig. 2. Representation of a rotoric loop

2.1.1 Voltage equations

Figure 2 depicts a segment of the equivalent electrical circuit of a rotor mesh, showcasing the rotor bars and short-circuit ring segments through their respective resistances and leakage inductances. Based on this illustration, the equations for the voltages of the three stator phases and the $(N_b + 1)$ rotor meshes can be derived. [21].

$$[V_s] = [R_s][I_s] + \frac{d[\psi_s]}{dt} \tag{1}$$

$$[V_r] = [R_r][I_r] + \frac{d[\psi_r]}{dt} \tag{2}$$

where $[\psi_s]$ and $[\psi_r]$ denote the vectors encapsulating the total fluxes through the stator and rotor windings, respectively. Meanwhile, $[I_s]$and $[I_r]$ represent the respective current vectors associated with these windings, as follows:

$$[\psi_s] = [L_{ss}][I_s] + [L_{sr}][I_r] \tag{3}$$

$$[\psi_r] = [L_{rs}][I_s] + [L_{rr}][I_r] \tag{4}$$

$$[V_s] = [V_{sA} \quad V_{sB} \quad V_{sC}] \tag{5}$$

$$[V_r] = \left[V_{r1}V_{r2} \dots \dots V_{rN_b}V_{re}\right]^T \tag{6}$$

$$[I_s] = [i_{sA} \quad i_{sB} \quad i_{sC}]^T \tag{7}$$

$$[I_r] = \left[i_{r1}i_{r2} \dots \dots \dots i_{rN_b}i_{re}\right]^T \tag{8}$$

Where i_{rj} and i_{re} are respectively the currents of the j^{th} rotor mesh and of the short-circuit ring. V_{rj} and $V_{re}$are the corresponding voltages with, for a cage rotor (short-circuited mesh), V_{rj} = 0 and $V_{re} = 0$; j=1.2,….. N_b .The resistor matrices are symmetric matrices. $[R_s]$ is a 3×3 matrix, while $[R_r]$ has $(N_b +$

$1) \times (N_b + 1)$ elements that can be reconstructed from the laws relating to electrical circuits.
By joining both of equations (1) and (2) into the same matrix equation, we arrive at:

$$[V] = [R][I] + \frac{d([L],[I])}{dt} \quad (9)$$

Which gives ,

$$[V] = [R][I] + [I] \cdot \frac{d\theta_r}{dt} \cdot \frac{d[L]}{d\theta_r} + [L] \cdot \frac{d[I]}{dt} \quad (10)$$

$$[V] = [R][I] + [I]\Omega_r \cdot \frac{d[L]}{d\theta_r} + [L]\frac{d[I]}{dt} \quad (11)$$

While,

$$[V] = \begin{bmatrix}[V_s]\\ [V_r]\end{bmatrix} \quad (12)$$

$$[U] = [V_{sA} \quad V_{sB} \quad V_{sC} \quad 0 \quad 0 \quad 0 \quad \cdots \quad 0 \quad 0]^T \quad (13)$$

$$[I] = \begin{bmatrix}[I_s]\\ [I_r]\end{bmatrix} \quad (14)$$

$$[I] = [i_{sA} \quad i_{sB} \quad i_{sC} \quad i_{r1} \quad i_{r2} \quad \cdots \quad i_{rN_b} \quad i_{re}], \quad (15)$$

And,

$$[R] = \begin{bmatrix}[R_s] & 0\\ 0 & [R_r]\end{bmatrix} \quad (16)$$

$$[L] = \begin{bmatrix}[L_{ss}] & [L_{sr}]\\ [L_{rs}] & [L_{rr}]\end{bmatrix} \quad (17)$$

2.1.2 Mechanical equations

Depending on the specific application for which the motor is intended, the mechanical equation of motion can be formulated as follows:

$$J_T \cdot \frac{d\Omega_r}{dt} + f_V\Omega_r = T_e - T_r \quad (18)$$

where:
J_T : total moment of inertia;
f_V : viscous friction coefficient;
T_e : electromagnetic torque;
T_r : resistant torque.
And after simplifications which finally give the expression of the electromagnetic torque.

$$T_e = \frac{1}{2} \cdot [I_s]^T \cdot \frac{d[L_{sr}]}{d\theta_r} \cdot [I_r] \quad (19)$$

2.1.3 System of differential equations

We can group the voltage equations and the mechanical equation into a single matrix representation to arrive at a condensed form [22]:

$$[U] = [B] \cdot [X] + [A] \cdot [\dot{X}] \quad (20)$$

The vector $[\dot{X}]$ is written as follows :

$$[\dot{X}] = [\mathrm{A}]^{-1} \cdot [U] - [\mathrm{A}]^{-1} \cdot [\mathrm{B}] \cdot [X] \quad (21)$$

We thus reveal the state vector $[X]$ and the vector $[U]$ containing the external quantities to the machine such as:

$$[U] = \begin{bmatrix}[V]\\ -T_r\\ 0\end{bmatrix} \quad (22)$$

$$[X] = \begin{bmatrix}[I]\\ \Omega_r\\ \theta_r\end{bmatrix} \quad (23)$$

With the definition of matrices A and B given by:

$$[\mathrm{A}] = \begin{bmatrix}\left([R] + \Omega_r \frac{d[L]}{d\theta_r}\right) & 0 & 0\\ -\frac{1}{2}[I]^T \frac{d[L]}{d\theta_r} & f_V & 0\\ 0 & -1 & 0\end{bmatrix} \quad (24)$$

$$[\mathrm{B}] = \begin{bmatrix}[L] & 0 & 0\\ 0 & J_T & 0\\ 0 & 0 & 1\end{bmatrix}. \quad (25)$$

2.2 Modeling of the IM with eccentricity fault

Inadequate machining or wear over time can result in the misalignment of the machine's central axis, leading to dynamic eccentricity. This causes the rotor to rotate around the stator axis, as illustrated in Figure (3). Such eccentricity issues significantly affect the machine's performance. Specifically, when the air gap varies, it alters both the machine's individual and mutual inductances. This poses a significant challenge for induction generators, particularly because this issue frequently arises [23].

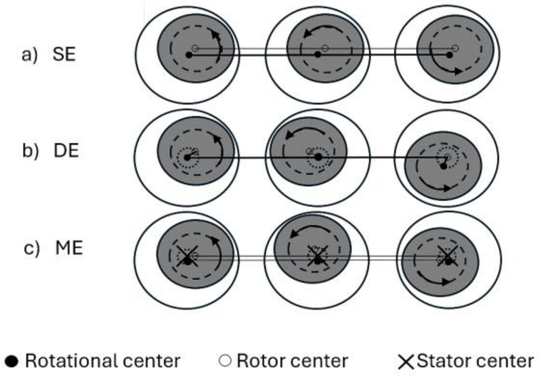

Fig. 3. Types of Eccentricities: a) static, b) dynamic and c) mixed

The third part of the IM is the air gap which is characterized by a void with a low thickness of 0.3 to 2mm, in general, this thickness is uniform (healthy state) between the rotor and the stator. However, it can be affected in the event of a fault of eccentricity. In induction machines, eccentricity refers to the misalignment of the rotor with respect to the stator axis. Eccentricity can occur in different forms, resulting in various types of eccentricity.

- *Static eccentricity*

SE simply changes the air gap configuration. In equation (26), where the air gap was originally consistent for a properly functioning machine, it now has a different value:

$$e_s(\theta_s) = e_0\left(1 - \delta_s \cdot \cos(\theta_s)\right) \quad (26)$$

δ_s: degree of static eccentricity.

- *Dynamic eccentricity*

This type is quite different from the previous type where the rotor now rotates around the stator bore center rather than its own center.

$$e_d(\theta_s) = e_0\left(1 - \delta_d \cdot \cos(\theta_s - \theta)\right) \quad (27)$$

δ_s: degree of the dynamic eccentricity

- *Mixed eccentricity*

Mixed eccentricity is the combination of the static air gap eccentricity and the dynamic one and its expression is as follows:

$$e_M(\theta_s, \theta) = e_0\big(1 - \delta_s \cdot \cos(\theta_s) - \delta_d \cdot \cos(\theta_s - \theta)\big) \quad (28)$$

The presence of eccentricity in induction machine has significant impacts on both the machine and personnel. It reduces machine efficiency, increases operating costs, decreases output performance, and accelerates wear and tear on components. Eccentricity requires more frequent maintenance, increases the risk of unplanned failures, and poses safety hazards. Personnel may face increased workloads, safety risks, and training requirements. Downtime and production losses can occur, and there is a risk of inaccurate diagnosis and inappropriate repair actions. Proactive measures, such as regular inspections and preventive maintenance, are essential to mitigate these influences, ensuring machine reliability, personnel safety, and optimal performance.

Figures (4) and (5) illustrate stator current signal for both a healthy and a faulty air gap under heavy load respectively. It can be noted that air gap eccentricity has a prominent influence on the sinusoidal form of the current on all of the phases in extreme degree of severity by causing undesirable oscillations and phase shift as can be shown, which indicates that eccentricity is a serious problem in IM that should put under a strong monitoring scope. Figure (6) on the other hand, indicate that early-stage air gap irregularity is hard to be detected in this stage, where oscillations can't be visible to the naked eye, which requires a supplementary analysis to put the fluctuations under investigation to make a proper decision about the machine's condition in order to prevent the deterioration of the machine's condition.

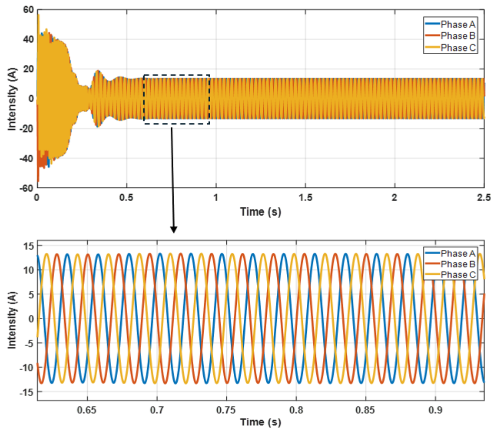

Fig. 4. Stator current under heavy load of a healthy air gap

To assess and diagnose the performance of our real model, a comprehensive analysis was conducted employing traditional approaches (MBMs) which include signal analysis techniques. This involved subjecting the model to spectral analysis utilizing FFT in the frequency domain. Additionally, an energy distribution analysis was performed using the WT approach, which operates in the time-frequency domain. These approaches were considered because they are extensively used in the diagnosis of IMs in hope to extract fault features across various operational scenarios and at different stages of defect severity.

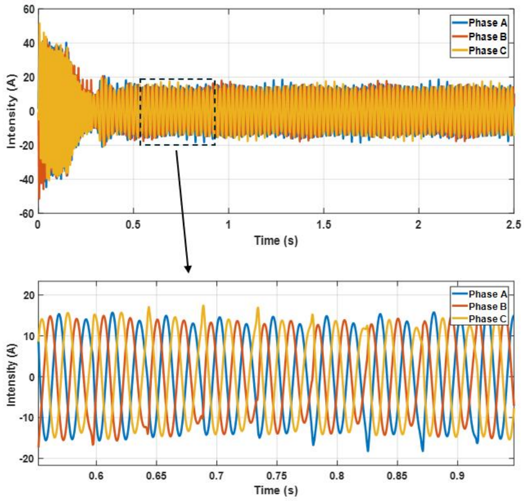

Fig. 5. Stator current under heavy load and mixed eccentricity

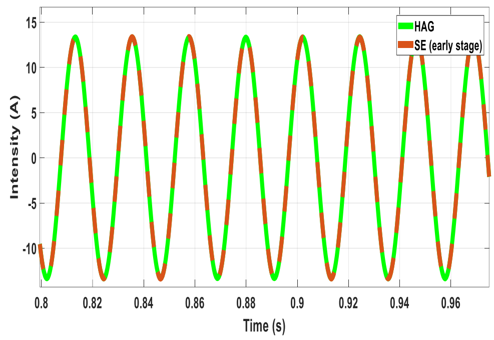

Fig. 6. Comparison of a healthy machine with an early stage of static eccentricity single phase stator current

Figures (7) and (8) show a spectral analysis of the stator current for both healthy and faulty air gap under weak load and for various stages of defect, it can be noted that FFT delivers useful information only in extreme stage of the defect, which is a drawback while performing a monitoring task.

After conducting the aforementioned diagnostic techniques, it becomes evident that the MBMs exhibit limitations, particularly when the IM is operating without a load or under weak load conditions. Additionally, these methods face challenges in detecting defects at early stages, where subtle fluctuations in the current pose difficulties. Moreover, their inadequacy extends to the identification of the nature of the defect (SE and ME), and also given that certain faults, such as bearing defects, broken rotor bars, and air gap eccentricity, manifest similar symptoms under weak load conditions, leading to potential misdiagnosis.

In scenarios where the IM operates with a small slip and rotational speed is in close proximity to synchronization, the frequencies associated with defects become challenging to discern due to their proximity to the fundamental frequency, coupled with their small amplitudes, which are situated in the side bands. This difficulty in detection is illustrated in Figure 9.

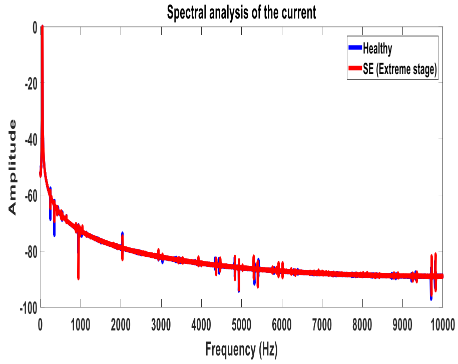

Fig. 7. Spectral analysis of static air gap eccentricity comparison under weak load conditions (healthy,early stage of airgap eccentricity)

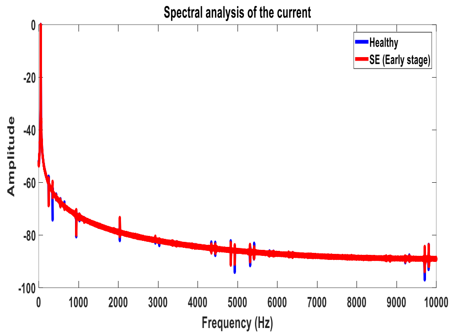

Fig. 8. Spectral analysis of static air gap eccentricity comparison under weak load conditions (healthy,extreme case of airgap eccentricity)

Furthermore, the limitations of MBMs extend to transient mode conditions, where spectral leakage becomes a significant issue. In situations where abrupt load fluctuations occur during operational conditions (e.g., in mills, wind turbines), these methods encounter challenges. The sudden changes in load cause distortion in the spectral image of the current, resulting in ambiguous frequencies. This distortion leads to a loss of information, as fault frequencies become obscured behind the frequency of load fluctuation. To address this issue and improve spectral resolution, longer measurement times are required, necessitating additional storage and sophisticated equipment.

It can be shown in Figure (10) that a full decomposition using (WT) was performed for both a healthy and faulty machine as a solution to mitigate the limitation of FFT technique by employing time and frequency domain analysis in order to have a better understanding of the signal's condition. However, when not treated with a proper investigation and extensive study, WT is limited while choosing the right mother wavelet to be implemented in the decomposition process, it can be computationally too extensive, WT has many variantes and each has its own advantage and drawback which requires a prior knowledge on the specified technique to be used

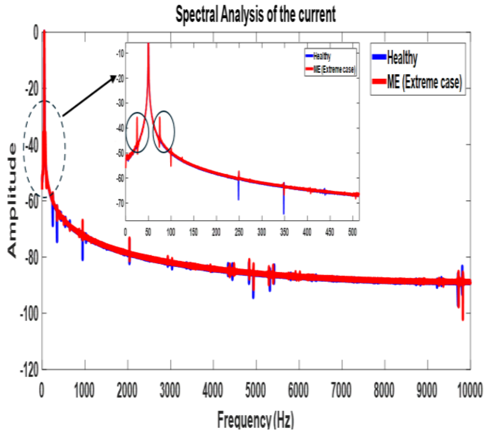

Fig. 9. Spectral analysis of Mixed air gap eccentricity comparison under weak load conditions (healthy,extreme cas.e of airgap eccentricity)

Figure (11) illustrates clearly the disadvantages of WT energy distribution technique, while performing feature extraction it requires a careful choice of decomposition level through all of the signals conditions (fault type,health condition and load's condition) so it can be suitable for the diagnosis task (see Figure 11a,b) it can be shown that a faulty machine dissipates more energy than the healthy model which is illogical and may lead to misinterpretaion that can render this technique unsuitable for this case.

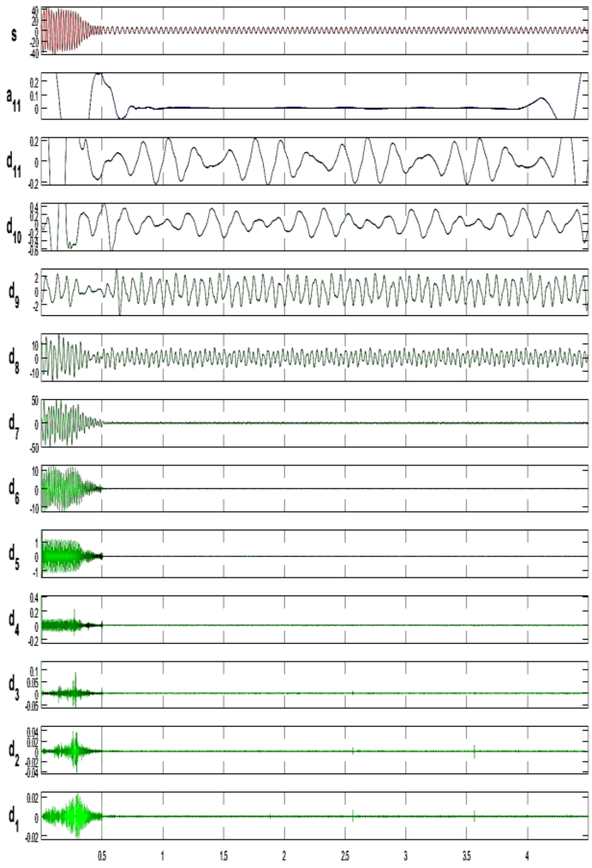

(a)

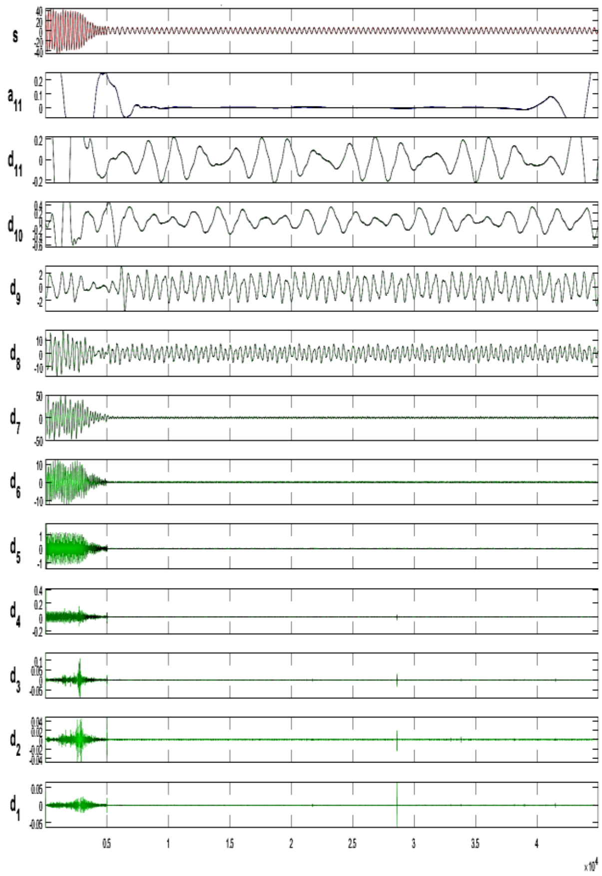

(b)

Fig. 10. Signal decomposition using wavelet transform : a-healthy;b-faulty

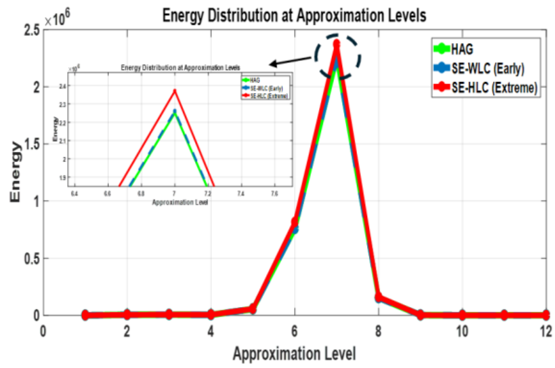

(a)

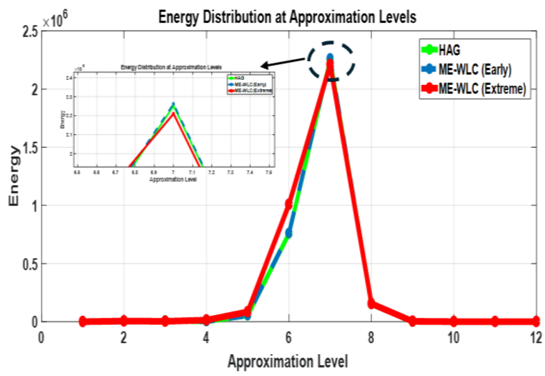

(b)

Fig. 11. Energy distribution analysis using WT at different stages under WLC: (a)-Healthy Vs Static eccentricity; (b) - Healthy Vs Mixed eccentricity

3. APPLICATION OF ARTIFICIAL INTELLIGENCE TECHNIQUES

An artificial neural network (ANN) is a machine learning technique designed to mimic the information processing capabilities of the human brain. In the human brain, neurons serve as the fundamental building blocks, with a single brain potentially containing between 15 to 20 billion of these interconnected cells. These neurons communicate through electrochemical signals, forming a complex network that facilitates various cognitive functions [24].

In a neural network, each neuron in a given layer receives input from every neuron in the preceding layer. Specifically, a feed-forward neural network operates without any feedback loops; it computes layer outputs exclusively through a forward pass. These feed-forward networks, especially those with multiple hidden layers referred to as deep neural networks can be shown in Figure 12 [25], are frequently employed for tasks like detecting faults in rotating machinery. The advantage of deep neural networks lies in their ability to learn intricate representations across multiple layers, enabling them to model complex relationships between input and target outputs.

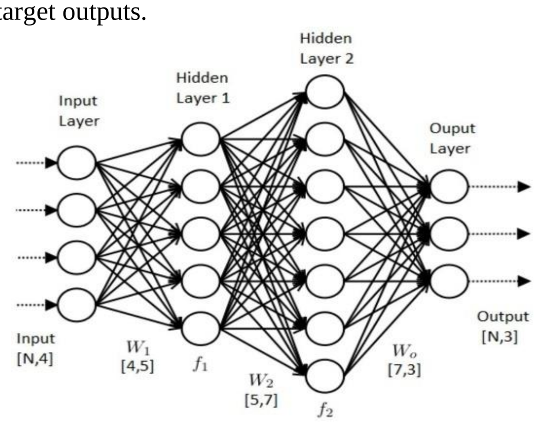

Fig. 12. MLP's network architecture

When applying neural networks to address the diagnosis of failures in an electromechanical system, two primary steps need to be implemented :

- The initial step involves examining the problem at hand to confirm its suitability for neural network-based solutions. This includes defining the objectives that need to be met to ensure the quality and effectiveness of the selected solution.
- The second step centers on the neural network technique. This involves selecting the appropriate network type and its configuration, such as determining the learning method and specifying the number of hidden layers. These choices are made based on the specific characteristics of the problem under investigation and the defined objectives.

The neural network was designed and trained to perform characterizations based on a database consisting of 216 samples. Each sample in the database contained 45,000 points representing the current signature, and the network aimed to predict four outputs related to the health state of the induction machine, the condition of the loads, and the designated stator current phase. For this phase the following tasks have been realized:

- The IM was simulated in ordinary operational conditions (healthy state);
- The IM has been simulated in abnormal operational conditions (in the presence of defects of air gap eccentricity in both types static and mixed);
- The IM has been simulated for both normal and abnormal for different working modes : low load torque (10N.m), medium load torque (30N.m) and high load torque (40N.m) as shown in Figure 13.

3.1 Classification of the machine's condition and fault nature

Selection of the outputs involves deciding on the number and type of outputs to simplify the interpretation of the network's results. The table 1 shows faults output classification.

Table 1. Fault's output classification

Machine condition	Load condition	Phase	Code S1	S2	S3	S4
HAG	WLC	Phase A	0	0	0	0
		Phase B	0	0	0	0.5
		Phase C	0	0	0	1
	MLC	Phase A	0	0	0.5	0
		Phase B	0	0	0.5	0.5
		Phase C	0	0	0.5	1
	HLC	Phase A	0	0	1	0
		Phase B	0	0	1	0.5
		Phase C	0	0	1	1
SE	WLC	Phase A	1	0	0	0
		Phase B	1	0	0	0.5
		Phase C	1	0	0	1
	MLC	Phase A	1	0	0.5	0
		Phase B	1	0	0.5	0.5
		Phase C	1	0	0.5	1
	HLC	Phase A	1	0	1	0
		Phase B	1	0	1	0.5
		Phase C	1	0	1	1
ME	WLC	Phase A	1	1	0	0
		Phase B	1	1	0	0.5
		Phase C	1	1	0	1
	MLC	Phase A	1	1	0.5	0
		Phase B	1	1	0.5	0.5
		Phase C	1	1	0.5	1
	HLC	Phase A	1	1	1	0
		Phase B	1	1	1	0.5
		Phase C	1	1	1	1

We end up by having 4 outputs containg 4 variables describing the machine parameters as follows:
S1: machine's health state;
S2: nature of air gap eccentricity (static or mixed);
S3: load's condition;
S4: stator current Phase.

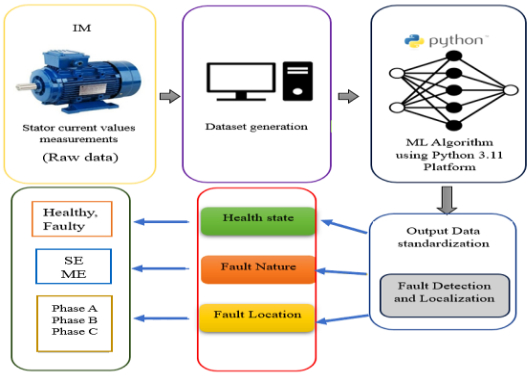

Fig. 13. Integration of the ML algorithm in the Diagnosis

4. RESULTS AND DISCUSSION

Classification techniques are employed for the identification and categorization of specific fault classes or operational states of the induction machine. Using historical data that includes normal and faulty machine behaviour, a classification model is trained to recognize patterns associated with different fault types. This enables the system to classify the current state of the machine into predefined categories, indicating the presence or absence of specific faults. Commonly used classification algorithms include neural networks, logistic regression, decision trees and support vector machines.

On the other hand, regression techniques are utilized for quantifying the severity or magnitude of faults detected in the induction machine. Unlike classification, regression models predict continuous numerical values, providing an estimate of the degree to which a fault has affected the machine's performance. Engineers use regression analysis to establish relationships between input features and the expected output, allowing them to assess parameters such as vibration levels, temperature variations, or other relevant indicators. Popular regression algorithms for induction machine diagnosis include linear regression, decision tree regression, and neural networks designed for regression tasks.

By combining classification and regression approaches, practitioners can create a robust diagnostic system that not only identifies the presence of faults but also provides insights into the extent of their impact on machine performance. This integrated approach enhances the reliability and accuracy of induction machine diagnostics, facilitating timely maintenance and minimizing downtime in industrial settings.

4.1 Classification technique

In the process of conducting the classification diagnosis, it is essential to note that alterations were made to the dataset's nature. Specifically, dataset transitioned from a set of continuous points representing the current sinusoidal signature to exclusive Root Mean Square (RMS) values. This modification aimed to enhance the suitability of utilizing labels crucial for this specific classification, ensuring that the dataset aligns optimally with the requirements of the classification task.

The classification process involved selecting RMS current values as predictors. To determine key attributes such as health state, fault type, load condition, and phase , they were chosen as response values , a 5-fold cross-validation method was applied. This technique partitions the dataset into five subsets for iterative training and validation, effectively avoiding overfitting risks.
As for the results are as follows in Figure 14 and table II.

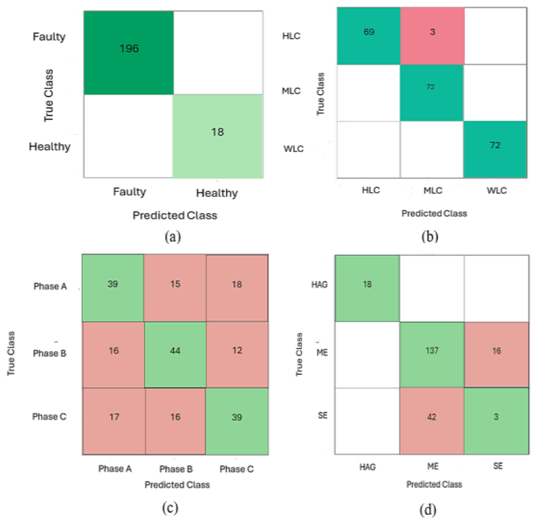

Fig. 14. Confusion matrix results: a-health state; b-load's condition; c-phase localization; d-fault's type

Table 2. Different machine learning classifiers performance

Preset	Fault detection	Fault identification	Load condition	Phase localization	Overall accuracy
Complex tree	100%	69.9%	97.7%	53.2%	80.2%
Medium tree	100%	72.7%	97.7%	53.2%	80.9%
Cubic SVM	100%	62.5%	98.6%	35.6%	74.1%
Fine Gaussian SVM	98.1%	75.5%	96.8%	20.4%	72.7%
Boosted trees	91.7%	69.9%	95.8%	52.8%	77.5%
RUSbossted trees	91.7%	42.6%	94.4%	49.1%	69.4%

Upon completing the classification task, it becomes evident that the Decision Trees classifier excels compared to the other selected classifiers, boasting an overall accuracy surpassing 80%. Specifically, by opting for the medium tree as its preset, it attained a commendable accuracy rate of 80.9%. This performance effectively enhances fault detection, fault identification, load condition assessment, and phase localization predictions.

4.2 Regression Technique

The second phase, regression approach was tested on raw dataset (a matrix of 216×45000) since It proves valuable in forecasting, hypothesis testing, and controlling for confounding variables, the interpretability of regression models also aids in pinpointing specific variables contributing to faults.

The chosen program utilizes the Random Forest Regressor from the scikit-learn framework to develop a regression prediction model. It begins by importing data from the provided raw dataset as inputs for features and the output from Table 1 as the target data. The dataset is then divided into training and test subsets in an 80:20 ratio (80% for training and 20% for test) to assess the model's efficiency on new data. Standardization of input features is performed using the StandardScaler to optimize the model training process. Following this, the Random Forest Regressor, comprised of 100 decision trees, is instantiated and trained on the standardized training dataset. Subsequent predictions are made for both the training and test sets.

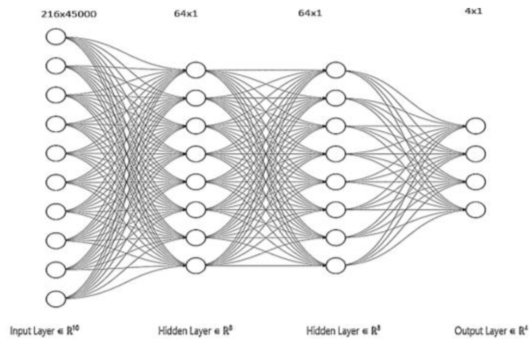

Fig. 15. The chosen network architecture

When assessing the effectiveness of regression methods, measures like Root Mean Square Error (RMSE), Mean Squared Error (MSE), and Mean Absolute Error (MAE) are extensively used to measure how closely predictions align with actual data. These measures offer a perspective on the suitability of a regression model to the dataset and the dependability of its forecasts.

4.2.1 Mean Squared Error

Mean Squared Error (MSE) calculates the average squared discrepancy between the actual and forecasted values within a dataset. Essentially, it quantifies the variability or dispersion of the residuals.

$$\mathrm{MSE} = \frac{1}{n}\sum_{i=1}^{n} (y_i - \hat{y}_i)^2 \tag{29}$$

n : number of observations;
y_i: actual value;
$\hat{y}_i$: predicted value.

4.2.2 Root Mean Square Error

It is derived by taking the square root of the Mean Squared Error. It serves as a metric for the standard deviation of the residuals.

$$\text{RMSE} = \sqrt{\frac{1}{n}\sum_{i=1}^{n}(y_i - \hat{y}_i)^2} \tag{30}$$

4.2.3 The Mean Absolute Error (MAE)

It calculates the average absolute variance between the real and forecasted values within a dataset. It quantifies the average magnitude of the residuals in the dataset.

$$\text{MAE} = \frac{1}{n}\sum_{i=1}^{n}|y_i - \hat{y}_i| \tag{31}$$

And the results of training the regressions models on the raw dataset and after evaluations using the previous metric are as follows in Table III.

Table 3. Regression Models Evaluation

Ml algorithm	Regression Model	MSE	RMSE	MAE
Supervised learning	Decision Trees	0.05813	0.24112	0.05813
	ElasticNet	0.1322	0.36359	0.31994
	KernelRidge	0.05365	0.23163	0.15355
	K-Nearest Neighbors (KNN)	0.05720	0.23918	0.10775
	Support Vector Machine (SVM)	0.04370	0.20906	0.13230
Ensemble Methods	Random Forest	0.01431	0.07336	0.16926
Neural Networks	Artificial neural Networks (ANN)	0.07595	0.27559	0.19438
	Long Short-Term Memory (LSTM)	0.2001	0.44742	0.39508

In contrast to various regression algorithms such as Artificial Neural Network (ANN), K-Nearest Neighbors (KNN), Support Vector Machine (SVM), Kernel Ridge, ElasticNet, Long Short-Term Memory (LSTM), and Decision Tree, Random Forest consistently demonstrated superior performance across key evaluation metrics. The thorough assessment highlighted Random Forest's proficiency in minimizing prediction errors, demonstrating its efficiency in capturing inherent patterns and relationships within the dataset. This finding emphasizes the reliability and effectiveness of the Random Forest algorithm in regression applications, establishing it as a compelling choice for accurate and dependable predictive modelling.
The Random Forest technique prediction results are as follows in Figures 16-19 and Figure 20 present Overall comparison of the regression models.

Fig. 16. Results of test predictions of the machine's health state

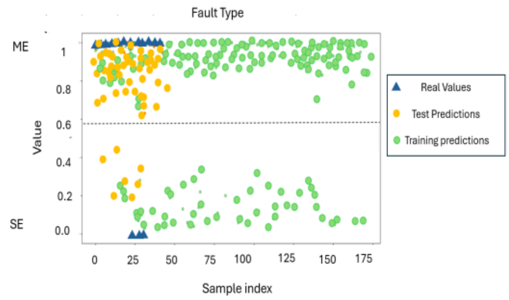

Fig. 17. Results of test predictions of the fault's Type

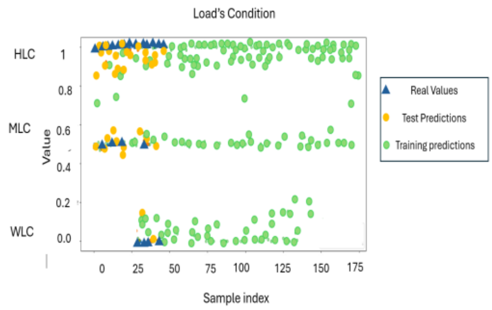

Fig. 18. Results of test predictions of the load's condition

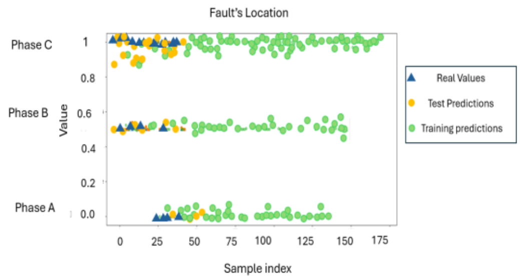

Fig. 19. Results of test predictions of the phase location

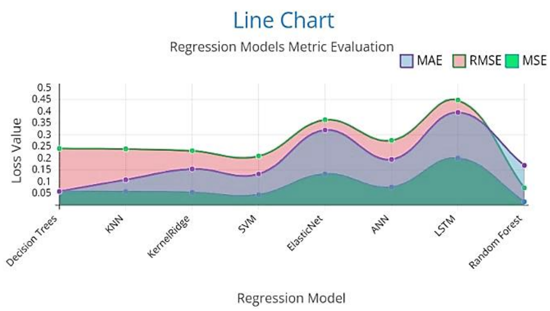

Fig. 20. Overall comparison of the regression models

5. CONCLUSION

After a thorough comparison of the classification task preset model and the regression task models for identifying air gap eccentricity faults in induction machines, both methods exhibit considerable potential. Yet, when using stator current raw data as inputs, the regression task model slightly outperforms in accuracy and precision. This slight advantage implies that regression methods might provide deeper understanding into the machine's health condition, pinpointing the exact type and location of faults, and assessing operational load conditions. Nonetheless, both strategies offer valid choices, and the selection should align with particular application needs and goals.

The upcoming work will focus on developing an algorithm capable of recognizing and predicting the degree of air gap eccentricity, considering its various types and load conditions. The primary objective is to enable effective monitoring at early stages of the defect of the machine's health status and prevent imminent dangers that could provoke undesirable breakdowns.

Source of funding: *This research received no external funding.*

Author contribution: *research concept and design, M.B.B., A.G.; Collection and/or assembly of data, M.M.B., A.G.; Data analysis and interpretation, M.M.B., A.G., T.B.; Critical revision of the article, A.G., T.B., Final approval of the article, A.G., T.B.*

Declaration of competing interest:
The authors declare that they have no known competing financial interests or personal relationships that could have appeared to influence the work reported in this paper.

REFERENCES

1. Glowacz A, Glowacz Z. Diagnosis of the three-phase induction motor using thermal imaging. Infrared Physics & Technology 2017;81:7–16. https://doi.org/10.1016/j.infrared.2016.12.003.
2. Hegde V, Maruthi GS. Experimental investigation on detection of air gap eccentricity in induction motors by current and vibration signature analysis using non-invasive sensors. Energy Procedia 2012;14:1047–52. https://doi.org/10.1016/j.egypro.2011.12.1053.
3. Subotic I, Dordevic O, Gomm JB, Levi E. Active and reactive power sharing between three-phase winding sets of a multiphase induction machine. IEEE Transactions on Energy Conversion 2019;34(3): 1401–10. https://doi.org/10.1109/TEC.2019.2898545.
4. Chuan H, Gan L. Investigation of the power losses in induction machines with rotor eccentricity. Electrical Engineering 2020; 102: 1–11. https://doi.org/10.1007/s00202-020-00957-0.
5. Khireddine MS, Slimane N, Abdessemed Y, Makhloufi MT. Fault detection and diagnosis in induction motor using artificial intelligence technique. MATEC Web of Conferences 2014;16. https://doi.org/10.1051/matecconf/20141610004.
6. Pradhan S, Bhowmik PS, Prakash M. Fault diagnostic and monitoring methods of induction motor: a review. International Journal of Applied Control, Electrical and Electronics Engineering 2013; 1: 1–18.
7. Ojaghi M, Mohammadi M. Unified modeling technique for axially uniform and nonuniform eccentricity faults in three-phase squirrel cage induction motors. IEEE Transactions on Industrial Electronics 2018; 65(7): 5292–301. https://doi.org/10.1109/TIE.2017.2760280.
8. Lee IS. Fault diagnosis of induction motors using discrete wavelet transform and artificial neural network. 2011; 173: 510–4. https://doi.org/10.1007/978-3-642-22098-2_102.
9. Ayhan B, Chow MY, Song MH. Multiple discriminant analysis and neural-network-based monolith and partition fault-detection schemes for broken rotor bar in induction motors. Industrial Electronics, IEEE Transactions on 2006;53:1298–308. https://doi.org/10.1109/TIE.2006.878301.
10. Senthil Kumar R, Gerald Christopher Raj I. Broken rotor bar fault detection using DWT and energy eigenvalue for DTC fed induction motor drive. International Journal of Electronics 2021;108(8): 1401–25. https://doi.org/10.1080/00207217.2020.1870727.
11. Abd-El-Malek M, Abdelsalam A, E. Hassan O. Induction motor broken rotor bar fault location detection through envelope analysis of start-up current using Hilbert transform. Mechanical Systems and Signal Processing 2017;93:332–50. https://doi.org/10.1016/j.ymssp.2017.02.014.
12. Rivera-Guillen JR, De Santiago-Perez JJ, Amezquita-Sanchez JP, Valtierra-Rodriguez M, Romero-Troncoso RJ. Enhanced FFT-based method for incipient broken rotor bar detection in induction motors during the startup transient. Measurement 2018;124:277–85. https://doi.org/10.1016/j.measurement.2018.04.039.
13. Pineda-Sanchez M, Puche-Panadero R, Riera-Guasp M, Perez-Cruz J, Roger-Folch J, Pons-Llinares J. Application of the teager–kaiser energy operator to the fault diagnosis of induction motors, 2013.
14. Ben Salem S, Salah M, Bacha K, Chaari A. Experimental investigation of the eccentricity impact on the line current spectrum for induction motors fault diagnosis purposes. 2016 17th International Conference on Sciences and Techniques of Automatic Control and Computer Engineering (STA) 2016: 205–10. https://doi.org/10.1109/STA.2016.7952070.
15. Reda R, Fayçal A, Tahar B. Fault eccentricity diagnosis in variable speed induction motor drive using DWT. Advances in Modelling and Analysis C 2017;72(3):181–202. https://doi.org/10.18280/ama_c.720301.
16. Al Tobi MAS, K P R, Al-Araimi S, Pacturan R, Rajakannu A, Achuthan G. Machinery fault diagnosis using continuous wavelet transform and artificial intelligence based classification. 2022 The 3rd International Conference on Robotics Systems and Vehicle Technology (RSVT) 2022:51–9. https://doi.org/10.1145/3560453.3560463.
17. Chouidira I, Khodja DE, Chakroune S. Induction machine faults detection and localization by neural networks methods. Revue d'Intelligence Artificielle 2019; 33(6): 427-434. https://doi.org/10.18280/ria.330604.
18. Saucedo-Dorantes JJ, Zamudio-Ramirez I, Cureno-Osornio J, Osornio-Rios RA, Antonino-Daviu JA. Condition monitoring method for the detection of fault graduality in outer race bearing based on vibration-current fusion, statistical features and neural network. Applied Sciences 2021;11(17):8033. https://doi.org/10.3390/app11178033.
19. Heming L, Liling S, Boqiang X. Research on transient behaviors and detection methods of stator winding

inter-turn short circuit fault in induction motors based on multi-loop mathematical model. Proceeding of IEEE ICEMS 2005;3:1951–1955.
20. Luo X, Liao Y, Toliyat H, El-Antably A, Lipo TA. Multiple coupled circuit modeling of induction machines. 1993;31:203–10. https://doi.org/10.1109/IAS.1993.298925.
21. Razik H, Didier G. Notes de cours sur le diagnostic de la machine asynchrone. Notes de cours, I.U.F.M. de Lorraine, Maxeville, 7 Janvier 2003.
22. Yassa N, Rachek M, Houssin H. Motor current signature analysis for the air gap eccentricity detection in the squirrel cage induction machines. Energy Procedia 2019;162:251-262.
23. Pelvig DP, Pakkenberg H, Stark A, Pakkenberg B. Neocortical glial cell numbers in human brain. Neurobiology of aging 2007;29:1754–62. https://doi.org/10.1016/j.neurobiolaging.2007.04.013.
24. Laudani A, Lozito GM, Riganti Fulginei F, Salvini A. On training efficiency and computational costs of a feed forward neural network: A review. Computational Intelligence and Neuroscience 2015; 2015(1):818243. https://doi.org/10.1155/2015/818243.
25. Gentili PL, Gotoda H, Dolnik M, Epstein I. Analysis and prediction of aperiodic hydrodynamic oscillatory time series by feed-forward neural networks, fuzzy logic, and a local nonlinear predictor. Chaos (Woodbury, N.Y.) 2015;25:013104. https://doi.org/10.1063/1.4905458.

Moutaz Bellah BENTRAD was born in ANNABA, on September 7, 1993, he is a PhD student in the Department of Electrical Engineering at Mohamed Khider Biskra University and affiliated to LGEB laboratory. He received the Electrical Engineering Electrical Commands master's degree in 2020 from the University of Badji Mokhtar Annaba. his research interests include condition monitoring and fault diagnosis in electrical machines.
e-mail: moutazbellah.bentrad@univ-biskra.dz

Adel GHOGGAL was born in Biskra, Algeria, in1971. He received the Engineer and Magister diploma and the Ph.D. degree in electrical engineering from the University of Biskra, in 1996, 2005 and 2010 respectively. Mr. Ghoggal is an assistant professor with the University of Biskra since 2005 and he is a member in the LGEB Laboratory. His research interests are focused on electrical machines design and fault diagnosis in power electronics systems and AC machines.
e-mail: a.ghoggal@univ-biskra.dz

Tahar BAHI Professor of Electrical Engineering, Member of the Annaba Automation and Signals Laboratory "LASA" Head of Degree: Industrial Electrical Engineering Head of the master's degree: control of industrial systems Responsible for Doctoral Studies: control of industrial systems and renewable energies. Member of the Synthesis journal editorial committee Member.
e-mail: tbahi@hotmail.fr